



OPEN Differences between suspected keratoconus and subclinical keratoconus via multiparameter analysis in Chinese populations

Yusu Peng¹, Qingqing Feng², Ting Shao¹, Jiafan Zhang¹, Sai Liu¹, Huifeng Wang¹, Hua Li¹ & Keli Long¹✉

Keratoconus (KC) is a contraindication for corneal refractive surgery and can cause serious damage to the patient's vision. To improve the safety of the surgery, we aim to distinguish between suspected KC and subclinical KC, while also developing a predictive model for KC. This cross-sectional study investigated 116 eyes with suspected KC (I-S Value > 1.4 D and ≤ 1.9 D) and 28 eyes with subclinical KC. All the Chinese subjects were examined via the Pentacam and Corvis ST (Oculus, Wetzlar, Germany). The 90 parameters of the Belin/Ambrósio System, Topometric/KC System, and Corvis ST System were extracted from internal CSV files and analyzed. The differences in all the parameters between the two groups were compared, and ROC curves were created. LASSO regression was employed to simplify the number of parameters, and a logistic regression model was constructed for KC prediction. The suspected KC group, in contrast to the subclinical KC group, predominantly consisted of females and older patients. The highest AUC parameters of the three systems were PachyProgIndexMax [0.896 (0.839, 0.954), cutoff = 1.445], IHD [0.787 (0.691, 0.883), cutoff = 0.029], SPA1 [0.811 (0.718, 0.904), cutoff = 87.485]. For the first discovery, the corneal diameter in the suspected KC group (11.56 ± 0.38) was smaller than that in the subclinical KC group (11.91 ± 0.33) ($P < 0.05$) [AUC = 0.736 (0.641, 0.832), cutoff = 11.825]. Seven relevant parameters were identified via LASSO regression (AUC = 0.954), including IHD, Cornea Diameter, DARatioMax_2 mm, BADDy, BADD, PachyProgIndexMax, and CBI. The prediction accuracy of the logistic regression model was 0.902 (AUC = 0.964). Our model effectively predicts an elevated risk of suspected KC to subclinical KC and even KC in younger Chinese men, particularly those exhibiting increased corneal diameter and morphological and biomechanical parameters. This model might help with screening for preoperative refractive surgery, thereby improving surgical safety.

Keywords Suspected keratoconus, Subclinical keratoconus, I-S value, Corneal diameter, Prediction model

Corneal refractive surgery is gradually becoming safer and more effective because of advancements in femtosecond and excimer laser technology. Before surgery, it has always been important to carefully determine the surgical indication¹. Keratoconus (KC) is recognized as a contraindication for corneal refractive surgery and poses a significant risk to the patient's vision. Therefore, it is crucial to conduct thorough screenings for patients who may exhibit signs of suspected keratoconus (refer to Fig. 1D). This condition is characterized by an abnormal steepening of the corneal topography, which may present as an asymmetric, truncated, or skewed-axis bowtie in the inferior focal area, while the fellow eye remains free of keratoconus² (Fig. 1C). Subclinical KC (Fig. 1B) shares a similar topographic asymmetry with suspected KC, although the fellow eye has KC³ (Fig. 1A) and may progress to KC⁴. Thus, it is especially crucial to identify individuals who may have KC before they experience visual loss or exhibit a positive slit-lamp test result.

The examination of corneal topography via various design principles is necessary to diagnose KC. The Pentacam can measure anterior and posterior corneal surface curvature and corneal thickness with accuracy via its unique Belin/Ambrósio system, whereas the Topometric/KC system shows significance in the diagnosis

¹Eye Institute of Shandong First Medical University, Qingdao Eye Hospital of Shandong First Medical University, State Key Laboratory Cultivation Base, Shandong Key Laboratory of Eye Diseases, School of Ophthalmology, Shandong First Medical University, 5 Yan'erdao Road Qingdao, Qingdao 266071, Shandong Province, China. ²Qingdao Central Hospital, University of Health and Rehabilitation Sciences, Qingdao, China. ✉email: longkeli2002@aliyun.com

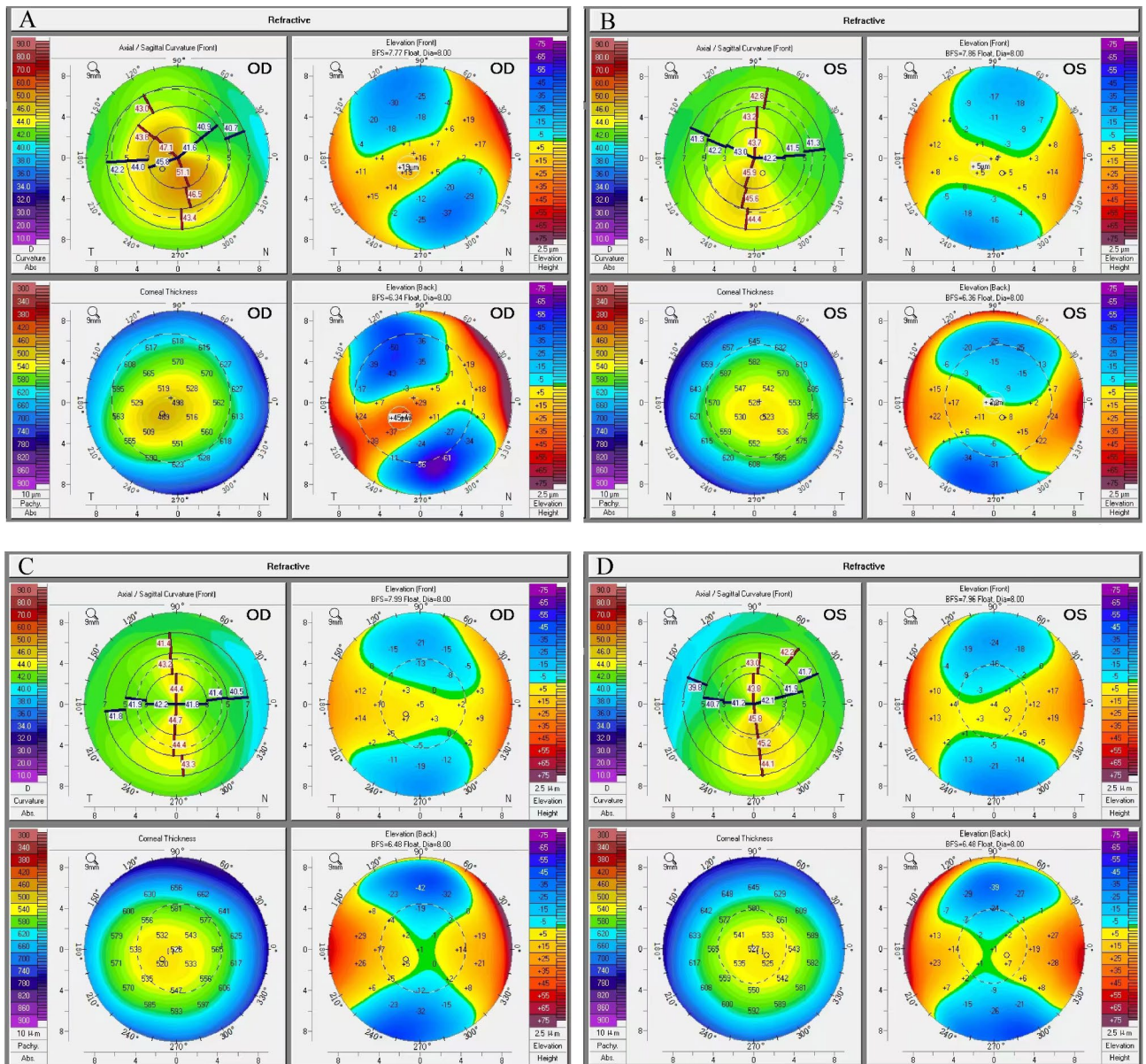


Fig. 1. Subclinical KC patient and Suspected KC patient. (A) Keratoconus(KC) eye, I-S Value = 1.73, BADD = 6.03; (B) Contralateral subclinical KC eye, I-S Value = 1.47, BADD = 1.93; (C) Normal eye, I-S Value = 1.08, BADD = 1.44; (D) Contralateral suspected KC eye, I-S Value = 1.61, BADD = 1.53.

of KC⁵⁻⁸. According to recent reports^{9,10}, KC can occur when corneal collagen fibers rupture in the early stages of the disease, and changes in corneal biomechanical characteristics occur earlier than changes in corneal morphological changes. Therefore, analyzing the combination of morphology and biomechanics via the Pentacam and Corvis ST to differentiate between KC and other conditions is a highly effective strategy¹¹⁻¹³.

An increasing number of artificial intelligence-related models, such as decision trees, random forests, and machine learning, have been found to be applicable in predicting KC¹⁴⁻¹⁷. Hu et al.¹⁸ employed UHR-OCT to produce thickness indices that demonstrated significant diagnostic effectiveness in differentiating between suspected and subclinical KC in comparison to normal eyes. However, there is limited diagnostic power in differentiating between suspected and subclinical KC, and there is insufficient research available to predict the probability of suspected KC advancing to subclinical or even KC. To thoroughly investigate the differences between suspected KC and subclinical KC, as well as to attempt to construct models of the correlation between them for prediction analysis, we extracted all of the detection-related original data from the Pentacam system and the Corvis ST system for this study.

Patients and methods

This study was approved by the Ethics Committee of Qingdao Eye Hospital of Shandong First Medical University. Approval was obtained following the principles outlined in the Helsinki Declaration. Each participant provided informed consent before their data were analyzed.

Inclusion and exclusion criteria for participants

Patients from the Qingdao Eye Hospital of Shandong First Medical University were recruited for this study. The criteria for patients in the suspected KC group included the following: normal slit-lamp examination (stromal thinning, Vogt's striae, Fleischer's ring); corrected distance visual acuity of 20/20 or better (Snellen); I-S Value $> 1.4D$ and $\leq 1.9D^{2,19}$; presence of yellow or red color-coded number (≥ 1.6 SD) in at least one of the five differential parameters (BADDf, BADDb, BADDp, BADDt, BADDa) in the Belin/Ambrósio Enhanced Ectasia Display; or white or yellow color-coded number in the final parameter "BADD"¹⁸; and follow-up for at least one year with no KC development. The criteria for inclusion of patients with subclinical KC were consistent with the abovementioned diagnostic criteria for suspected KC in terms of corrected distance visual acuity, slit-lamp examination, I-S Value, and topographic signs, with KC in fellow eyes³.

The exclusion criteria included individuals who had worn corneal contact lenses for less than 4 weeks (for hard contact lenses) or less than 2 weeks (for soft contact lenses); individuals with a history of eye diseases such as cataracts, retinal detachment, or mild corneal endothelial dystrophy; individuals with moderate to severe dry eyes or high intraocular pressure (IOP); individuals with scar constitution; and individuals who were pregnant or lactating.

Ophthalmology-related examination

The basic data of the patients, including their sex and age, were collected.

Corneal morphological parameters: A total of fifty-five original parameters (using internal CSV files) were collected via the Belin/Ambrósio system and the Topometric/KC system via the Pentacam anterior segment analysis system (Oculus, Germany). These included fifteen Belin/Ambrósio system parameters, such as K1, K2, Astigm, BADDf, BADDb, BADDp, BADDt, BADDa, BADDy, BADD, PachyProgIndexMin, PachyProgIndexMax, PachyProgIndexAvg, ARTMax, DistApexThinLoc; 40 Topometric/KC system parameters: CorneaDia, RSagMin, ISV, IVA, KI, CKI, IHA, IHD, D0 mmPachy, D2 mmPachy, D4 mmPachy, D6 mmPachy, D8 mmPachy, D2 mmStdDev, D4 mmStdDev, D6 mmStdDev, D8 mmStdDev, CVolD3 mm, CVolD5 mm, and CVol. D7 mm, KMaxFront, MaxZonalMean3 mm, KMaxZonalMean4 mm, KMaxZonalMean5 mm, I-S Value, PRC3 mmZone, ARC3 mmZone, ThinnestPachy, ChordMu.polarvector, ABCDA, ABCDB, ABCDC, IrisConvexityMid, IrisConvexityMax, IrisConvexityAxisMax, IrisConvexityMin, IrisConvexityAxisMin, Rf, Rs, CFSagZonalMean4 mm.

The corneal biomechanical parameters included the following: the biomechanical parameters of the cornea were assessed via a Corvis ST Corneal Biomechanics Meter (Oculus, Wetzlar, Germany) following a 20 min Pentacam examination for each patient. Thirty-five parameters were collected from the system's original data (internal CSV file), including A1Time, A1Velocity, A2Time, A2Velocity, HCTime, PeakDist, A1DeformationAmp, A2DeformationAmp, A1DeflectionLength, HCDeformationAmp, HCDeflectionLength, A2DeflectionLength, A1DeflectionAmp, HCDeflectionAmp, A2DeflectionAmp, DeflectionAmpMax_mm, DeflectionAmpMax_ms, A1DeflectionArea, HCDeflectionArea, A2DeflectionArea, A1dArcLength, HCdArcLength, A2dArcLength, dArcLengthMax, MaxInverseRadius, Radius, PachySlope, DefAmpMax, DARatioMax2 mm, IntegratedRadius, DARatioMax1 mm, ARTh, SPA1, CBI.

Statistical methods

All continuous variables were assessed for normality via the Shapiro-Wilk test. Normally distributed variables were reported as the means \pm SDs ($\bar{x} \pm s$), with group comparisons performed via t-tests. Skewed variables were described by the median and interquartile range (M (P25, P75)), and differences between groups were analyzed by the Wilcoxon rank sum test. Categorical variables were presented as constituent ratios (%), with chi-square tests used for intergroup comparisons.

ROC analysis was performed on various parameters of the Belin/Ambrósio system, Topometric/KC system, and Corvis ST system for the suspected KC group and the subclinical KC group. The best cutoff value was selected as the most approximate index.

After the continuous variables from the three systems were normalized and the categorical variables were encoded into dummy variables, a mathematical prediction model was established via LASSO regression to differentiate between the suspected KC and subclinical KC populations. Through 10-fold cross-validation, the λ with the minimum mean error and λ (1 se) were obtained. A logistic regression-based mathematical prediction model was constructed based on the parameters selected by λ (1 se). The diagnostic performance of the mathematical model was evaluated via the area under the receiver operating characteristic curve (AUC), accuracy, sensitivity, and specificity.

All the statistical analyses were carried out via R studio (version 4.4.0), and the difference was determined as statistically significant when $P < 0.05$.

Results

Analysis of basic patient data

A total of 144 persons (144 eyes) were included in this study.

Approximately 72 (62.1%) of the 116 individuals (116 eyes) in the suspected KC group were female, and 44 (37.9%) were male, with an average age of 25.00 (20.00, 29.00). The subclinical KC group consisted of 28 people

(28 eyes), with an average age of 21.00 (17.75, 24.00) years. Nine (32.1%) of them were female, and 19 (67.9%) were male.

Parameter difference analysis of the two groups in the Belin/Ambrósio system, the Topometric/KC system, and the Corvis ST system

Eleven of the 15 (73.3%) Belin/Ambrósio system parameters ($P < 0.05$) were significantly different between the suspected KC group and the subclinical KC group, including BADDb, BADDp, BADDt, BADDa, BADDy, BADD, PachyProgIndexMin, PachyProgIndexMax, PachyProgIndexAvg, ARTMax, and DistApexThinLoc. Furthermore, 19 out of 40 (47.5%) Topometric/KC system parameters ($P < 0.05$), including Cornea Diameter, IVA, IHA, IHD, D0mmPachy, D2mmPachy, D4mmPachy, D8mmPachy, D2mmStdDev, D4mmStdDev, D6mmStdDev, D8mmStdDev, CVolD3mm, CVolD5mm, CVolD7mm, PRC3mm.Zone, ThinnestPachy, ABCDB, and ABCDC, were significantly different between the suspected KC group and the subclinical KC group. Finally, 9 out of 34 (26.5%) Corvis ST system parameters ($P < 0.05$) were significantly different between the suspected KC group and the subclinical KC group, including A1Time, A1DeformationAmp, DARatioMax_2mm, Integrated Radius, DARatioMax_1mm, ARTh, SPA1, and CBI (Table 1).

Assessment of the diagnostic power of the two groups under the AUC of the Belin/Ambrósio system, Topometric/KC system, and Corvis ST system

The Belin/Ambrósio system was used to differentiate between the suspected KC group and the subclinical KC group, and 8 out of 15 parameters had an AUC greater than 0.7 ($P < 0.05$). These parameters included PachyProgIndexMax [0.896 (0.839, 0.954, cutoff = 1.445), ARTMax [0.894 (0.838, 0.951), cutoff = 377.000], BADDa [0.893 (0.836, 0.950), cutoff = 1.010], BADD [0.878 (0.817, 0.939), cutoff = 1.980], BADDp [0.811 (0.730, 0.892), cutoff = 1.935], PachyProgIndexAvg [0.811 (0.730, 0.892), cutoff = 1.185], BADDy [0.758 (0.667, 0.848), cutoff = 0.745], BADDb [0.747 (0.648, 0.847), cutoff = 0.525]. Moreover, we found that 7 of the 40 Topometric/KC system parameters had an AUC greater than 0.7 ($P < 0.05$), including the D6mmStdDev. Finally, 4 of the 35 Corvis ST system parameters had an AUC greater than 0.7 ($P < 0.05$), including SPA1 [0.811 (0.718, 0.904), cutoff = 87.485], DARatioMax_2 mm [0.784 (0.691, 0.878), cutoff = 4.710], CBI [0.771 (0.657, 0.885), cutoff = 0.278], DARatioMax_1 mm [0.750 (0.653, 0.847), cutoff = 1.584] (Table 2; Fig. 2).

Screening of sensitive variables via LASSO Regression and Establishment of a logistic regression prediction model

The characteristics of the suspected and subclinical KC populations were screened via LASSO regression. All quantitative parameters were normalized, and categorical variables were set as dummy variables. Variables were screened, and a LASSO regression was created via tenfold cross-validation. Then, $\lambda_{\min} = 0.009$ and $\lambda_{1se} = 0.064$ were obtained. We then used λ_{1se} to construct a LASSO regression and eliminated the following variables: BADDy, BADD, Cornea Diameter, IHD, DARatioMax_2 mm, CBI, and PachyProgIndexMax (Fig. 3; Table 3).

The AUC (95% CI) of the LASSO regression based on the variables listed above was 0.954 (0.921, 0.986); the sensitivity was 0.905; the specificity was 1.000; and the accuracy was 0.908.

Based on the variables selected by LASSO regression, the following logistic regression equation was established:

$$\begin{aligned} \text{logit}(\text{Risk Score}) = \log(p/(1-p)) = & -62.18 + 243.19 \times \text{IHD} + 3.06 \times \text{Cornea Diameter} + 2.62 \\ & \times \text{DARatioMax_2mm} + 1.29 \times \text{BADDy} + 1.23 \times \text{BADD} + 1.03 \\ & \times \text{PachyProgIndexMax} + 0.68 \times \text{CBI} \end{aligned}$$

Suspected and subclinical KC were assessed via the risk score derived from the logistic model; the AUC (95% CI) was 0.964 (0.938, 0.991). The sensitivity and specificity were 0.888 and 0.963, respectively, and the accuracy was 0.902 (Fig. 4).

Discussion

Epidemiological research indicates that the incidence of keratoconus in the global population affects approximately 0.05% of people²⁰. The onset usually occurs at or around the age of 20. Males in Asian populations typically experience disease onset earlier and experience a faster rate of progression than females²¹, which is in line with the findings from the subclinical KC group in this study.

In this study, we found that, even within the same asymmetrical corneal population, there were morphological and biomechanical differences between the suspected and subclinical KC groups. When comparing the fraction of parameter differences, Pentacam outperformed Corvis ST, particularly for the Belin/Ambrósio system (73.3%). The sensitivity of a single parameter in each system was not very high. PachyProgIndexMax (0.896) and ARTMax (0.894) were the two largest AUCs of the parameters in the Belin/Ambrosio System. These values were higher than those reported in studies conducted by Awad et al.²² and Orkun Muftuoglu. et al.⁸ compared forme fruste keratoconus eyes to normal eyes (0.64, 0.88; 0.679, 0.772), but the results were lower than those of Vázquez et al. (0.92, 0.93)²³ because the majority (85.7%) of the control group they chose had normal map morphology.

Additionally, we discovered that the Belin/Ambrósio deviation correlation parameters (BADDa, BADDb, BADDp, BADDy, and BADD) also had high diagnostic values (AUC = 0.893, 0.747, 0.811, 0.745). It was previously acknowledged that a BADD > 1.6 SD was abnormal²³. However, this study discovered that to differentiate between the suspected and subclinical KC groups, BADD > 1.98 SD was considered abnormal. The primary cause of this discrepancy is due to previous studies comparing corneas with normal eyes^{16,24}. The

		Subclincial KC (N=28)	Suspected KC (N=116)	P
Basic parameters	Age	21.00 (17.75, 24.00)	25.00 (20.00, 29.00)	0.005 [*]
	sex(%)			
	Female	9 (32.1%)	72 (62.1%)	0.008 [*]
	Male	19 (67.9%)	44 (37.9%)	
Belin/Ambrósio System	BADDb	1.15 (0.74, 1.83)	0.14 (-0.26, 0.90)	<0.001
	BADDp	2.26 (1.33, 2.91)	1.07 (0.37, 1.62)	<0.001
	BADDt	0.94 ± 0.98	0.24 ± 0.82	0.001
	BADDa	1.81 ± 0.52	0.73 ± 0.73	<0.001
	BADDy	1.55 ± 0.81	0.67 ± 0.99	<0.001
	BADD	2.61 ± 0.73	1.56 ± 0.63	<0.001
	PachyProgIndexMin	0.88 ± 0.20	0.75 ± 0.14	0.004
	PachyProgIndexMax	1.78 (1.61, 1.94)	1.32 (1.18, 1.46)	<0.001
	PachyProgIndexAvg	1.24 (1.10, 1.34)	1.07 (0.96, 1.14)	<0.001
	ARTMax	289.54 ± 56.31	408.36 ± 79.91	<0.001
	DistApexThinLoc	0.77 (0.61, 0.91)	0.61 (0.44, 0.78)	0.004
Topometric/KC System	Cornea Diameter(mm)	11.88 ± 0.34	11.57 ± 0.40	<0.001
	IVA	0.28 (0.26, 0.30)	0.24 (0.22, 0.26)	<0.001
	IHA	17.45 (10.15, 23.58)	13.15 (5.10, 19.83)	0.037
	IHD	0.03 (0.03, 0.03)	0.02 (0.02, 0.03)	<0.001
	D0mmPachy(μm)	508.71 ± 29.66	531.16 ± 28.22	<0.001
	D2mmPachy(μm)	520.43 ± 29.78	540.34 ± 28.25	0.003
	D4mmPachy(μm)	554.43 ± 31.02	569.90 ± 29.11	0.021
	D8mmPachy(μm)	688.86 ± 37.63	705.59 ± 34.48	0.038
	D2mmStdDev	3.00 (2.00, 4.00)	2.00 (2.00, 2.00)	<0.001
	D4mmStdDev	13.00 (9.75, 15.00)	8.00 (6.00, 10.25)	<0.001
	D6mmStdDev	25.00 (19.75, 28.25)	16.00 (12.00, 20.00)	<0.001
	D8mmStdDev	41.00 (30.75, 48.00)	27.00 (21.00, 35.00)	<0.001
	CVolD3mm	3.75 (3.60, 3.90)	3.90 (3.70, 4.00)	0.006
	CVolD5mm	10.98 ± 0.64	11.36 ± 0.59	0.007
	CVolD7mm	23.77 ± 1.37	24.51 ± 1.26	0.013
	PRC3mm.Zone	6.10 ± 0.27	6.27 ± 0.20	0.004
	ThinnestPachy(μm)	508.71 ± 29.66	531.13 ± 28.21	<0.001
	ABCDB	0.15 (0.00, 1.00)	0.00 (0.00, 0.10)	0.003
ABCDC	0.65 (0.40, 1.10)	0.50 (0.10, 0.70)	0.002	
Corvis ST System	A1Time(ms)	7.37 (7.09, 7.51)	7.49 (7.30, 7.66)	0.006
	A1DeformationAmp	0.14 ± 0.01	0.14 ± 0.01	0.009
	DARatioMax_2mm	5.02 (4.66, 5.18)	4.47 (4.23, 4.78)	<0.001
	Integrated Radius	8.80 ± 1.00	8.24 ± 1.15	0.014
	DARatioMax_1mm	1.62 (1.60, 1.65)	1.58 (1.55, 1.61)	<0.001
	ARTh	402.74 (339.83, 492.15)	470.35 (404.09, 561.28)	0.007
	SPA1	81.46 (76.62, 86.84)	99.55 (87.51, 108.80)	<0.001
	CBI	0.77 (0.22, 0.97)	0.02 (0.00, 0.40)	<0.001

Table 1. Difference of all parameters between the subclincial KC group and suspected KC group. Values were presented as mean ± standard deviation, counts (M (P25, p75)) and percentages (%); N was presented as sample quantity; Parameters with $P < 0.05$ were selected to be included in the table.

control group selected in this study had asymmetric subclinical KC, and the BADD in some cases was observed to be more than 1.6 SD, which may be the reason for the high BADD cutoff value in this study.

According to our analysis of the Topometric/KC system, IHD, and IVA were the most correlated parameters in terms of marginal corneal dilatation, KC, and irregular astigmatism (AUC=0.787, 0.762). The greater the degree of vertical asymmetry of the cornea, the greater the likelihood of KC development^{25,26}. Both IHD and IVA significantly increased the progression of subclinical KC (AUC=0.855, 0.842) after one year of follow-up. et al.²⁷. This finding was consistent with that of the present study, suggesting that IHD and IVA could be used as crucial markers of the development of KC.

The corneal diameter in the subclinical KC group (11.88 ± 0.34) was surprisingly greater than that in the suspected KC group (11.56 ± 0.38). With a lower sensitivity (0.607) but a higher specificity (0.784), the AUC

	Variable	Cutoff	AUC(95%CI)	ACC	SEN	SPE	P
Belin/Ambrósio System	PachyProgIndexMax	1.455	0.896 (0.839, 0.954)	0.778	0.929	0.741	0.000*
	ARTMax	377.000	0.894 (0.838, 0.951)	0.729	0.672	0.964	0.000*
	BADDa	1.010	0.893 (0.836, 0.950)	0.722	0.964	0.664	0.000*
	BADD	1.980	0.878 (0.817, 0.939)	0.799	0.893	0.776	0.000*
	BADDp	1.935	0.811 (0.730, 0.892)	0.812	0.643	0.853	0.000*
	PachyProgIndexAvg	1.185	0.811 (0.730, 0.892)	0.799	0.643	0.836	0.000*
	BADDy	0.745	0.758 (0.667, 0.848)	0.646	0.929	0.578	0.000*
	BADDb	0.525	0.747 (0.648, 0.847)	0.674	0.821	0.638	0.000*
Topometric/KC System	D6mmStdDev	23.500	0.809 (0.717, 0.901)	0.847	0.607	0.905	0.000*
	IHD	0.029	0.787 (0.691, 0.883)	0.847	0.500	0.931	0.000*
	D4mmStdDev	11.500	0.783 (0.680, 0.886)	0.812	0.607	0.862	0.000*
	IVA	0.255	0.762 (0.666, 0.858)	0.646	0.786	0.612	0.000*
	D8mmStdDev	42.500	0.757 (0.658, 0.856)	0.826	0.500	0.905	0.000*
	D2mmStdDev	2.500	0.744 (0.652, 0.837)	0.736	0.607	0.767	0.000*
	Cornea Diameter	11.825	0.736 (0.641, 0.832)	0.750	0.607	0.784	0.000*
	Corvis ST System	SPA1	87.485	0.811 (0.718, 0.904)	0.755	0.750	0.778
DARatioMax_2mm		4.710	0.784 (0.691, 0.878)	0.713	0.741	0.707	0.000*
CBI		0.278	0.771 (0.657, 0.885)	0.734	0.741	0.733	0.000*
DARatioMax_1mm		1.584	0.750 (0.653, 0.847)	0.573	0.889	0.500	0.000*

Table 2. Assessment of the diagnostic ability of the two groups under the AUROC of the three systems. ACC: accuracy; SEN: sensitivity; SPE: specificity. Parameters with AUC > 0.7 were selected to be included in the table.

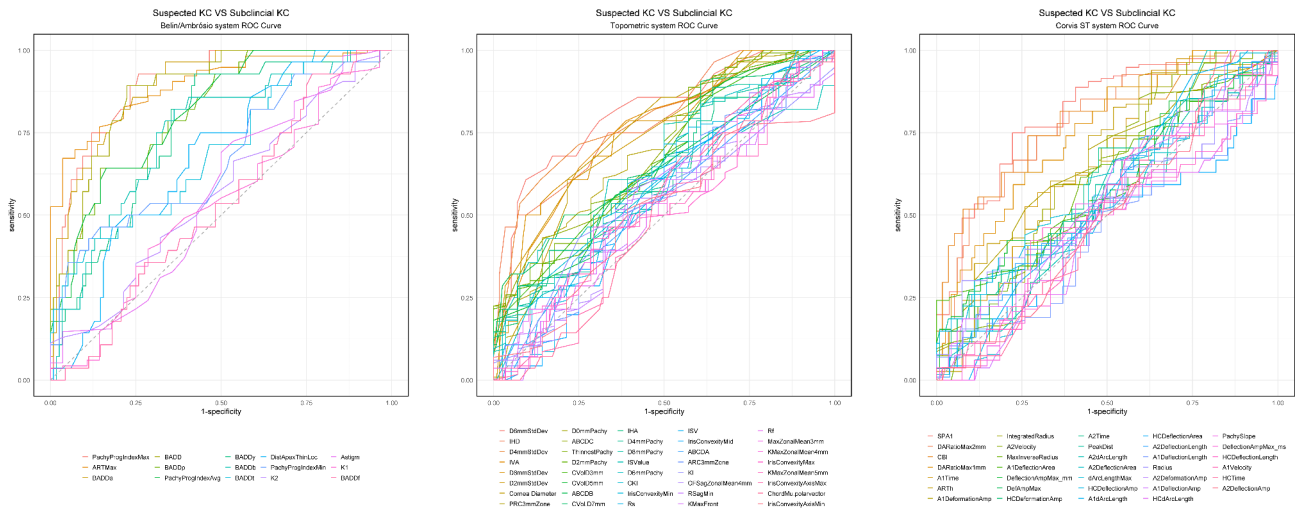


Fig. 2. ROC curve of Belin/Ambrósio system, Topometric/KC system and Corvis ST system between the two groups.

was 0.736 (0.641, 0.832), and the cutoff value was 11.825. Currently, there are significant differences in corneal diameter measurements from country to country. Alfonso JF. et al.²⁸ measured the corneal diameter of myopic individuals via Orbscan TM and reported that it ranged from 10.40 to 13.60 mm, whereas it ranged from 11.50 to 12.30 mm for emmetropia individuals found by Sanchis-Gimeno, J. A et al.²⁹ The corneal diameter of healthy individuals measured with the IOL Master 700 was 11.72 ± 0.45 mm. The corneal diameter of the Chinese myopic population was measured by Xu G. et al.³⁰ via Pentacam, and the result was 11.65 ± 0.38 mm, which was consistent with the results from the suspected KC group (11.56 ± 0.38 mm) in our study. The corneal diameter was found to be greater in both KC and contralateral eyes (12.14 mm and 12.17 mm), according to research by François-Xavier Crahay et al.³¹. The corneal diameter we measured in the subclinical KC group was not as large as that measured by François-Xavier Crahay because the corneal diameter and shape of the white population differ from those of the Chinese population^{32,33}. However, the KC population we studied had a larger corneal diameter. Thus, corneal diameter may be a crucial parameter for differentiating corneas in KC patients from those in the normal group.

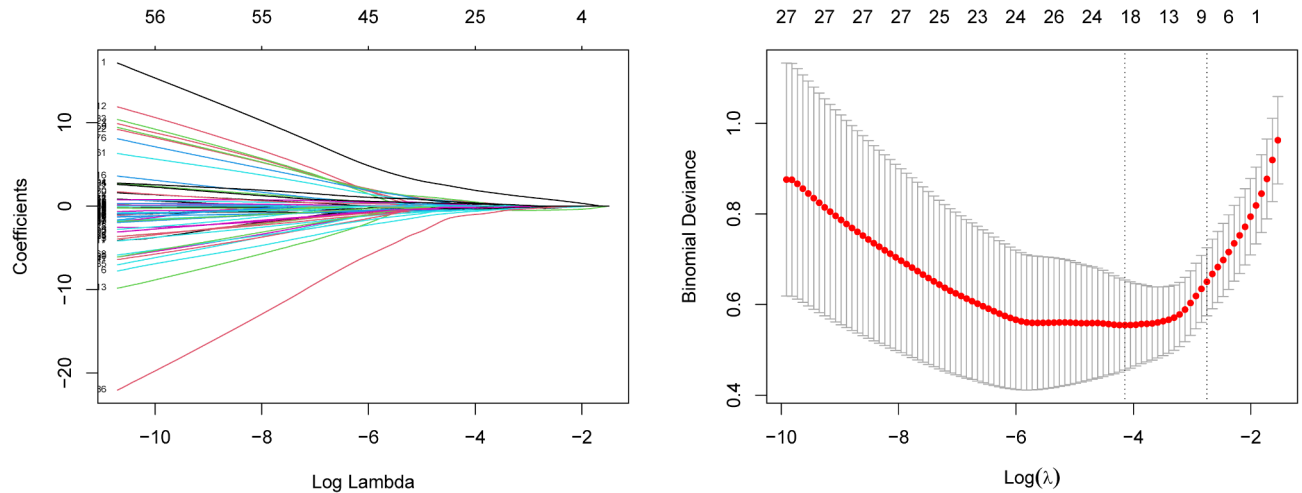


Fig. 3. Coefficient path plot of variables screened by LASSO regression.

Variable	Coefficient
intercept	1.78937717
BADDy	-0.0740568
BADD	-0.299099
PachyProgIndexMax	-0.4744784
Cornea Diameter	-0.2527814
IHD	-0.2887178
DARatioMax2mm	-0.1781822
CBI	-0.1117249

Table 3. Variables and coefficients selected by the LASSO regression.

The use of biomechanical examination is still vital in differentiating between KC and healthy corneas^{16,34}. In this study, we found that 26.5% of the Corvis ST system parameters differed between the two groups. The highest AUC values were found for SPA1 (0.811), DARatioMax_2mm (0.784), CBI (0.771), and DARatioMax_1mm (0.750). No parameter had a particularly high diagnostic efficacy, but this is subject to future research.

Racial differences in ocular parameters are critical for disease diagnosis, extending beyond corneal diameter to biomechanical metrics. Research conducted by Liu, Yan et al.³⁵ and Guo, Li-Li et al.³⁶ documented elevated false-positive rates of the CBI within Chinese populations. Vinciguerra, Riccardo et al.³⁷ highlighted disparities in SPA1, SSI, and ARTH between Chinese and Caucasian populations, subsequently introducing the cCBI, which outperformed CBI in diagnosing keratoconus in Chinese individuals. Additionally, Guo, Yihan et al.³⁸ revealed variations in the age-biomechanics relationship between these populations. This study focuses on Chinese samples, limiting its applicability to other ethnicities. Future multicenter, multiethnic studies are needed to confirm these findings.

No parameter in our work has an AUC of more than 0.9 because KC, especially in its early stages, cannot be diagnosed with a single parameter; rather, a comprehensive analysis necessitates the combination of multiple characteristics. Therefore, we developed a LASSO regression prediction model, which was first suggested in 1996 by Robert Tibshirani³⁹. This method of compressed estimation is used here. It produces a more refined model by building a penalty function that compresses some coefficients and sets others to zero. Complex collinear data are specifically designed to be handled by this biased estimation. There were 92 parameters in this study; however, there may have been connections between the parameters. We chose seven parameters via LASSO regression. AUC = 0.964 indicates that the logistic regression model based on the seven parameters has increased diagnostic power, effectively resolving the issue that prior studies were unable to differentiate between suspected and subclinical KC¹⁸.

Currently, a large body of research using artificial intelligence to predict the progression of keratoconus has been conducted^{14,15,17,40,41}, with good diagnostic power. For the first time, we used the internal parameters of the examination system to compare the differences between the two types of asymmetrical corneas in our study, and the result was a more precise prediction model. The results of our analysis of the samples we used in this model showed that IHD had the largest coefficient, indicating the strongest correlation with the development of the KC. We then studied the corneal diameter, DARatioMax_2mm, BADDy, BADD, PachyProgIndexMax, and CBI. The logistic regression model's AUC was 0.964, which was greater than that of studies of sequences 1 (0.849), 2

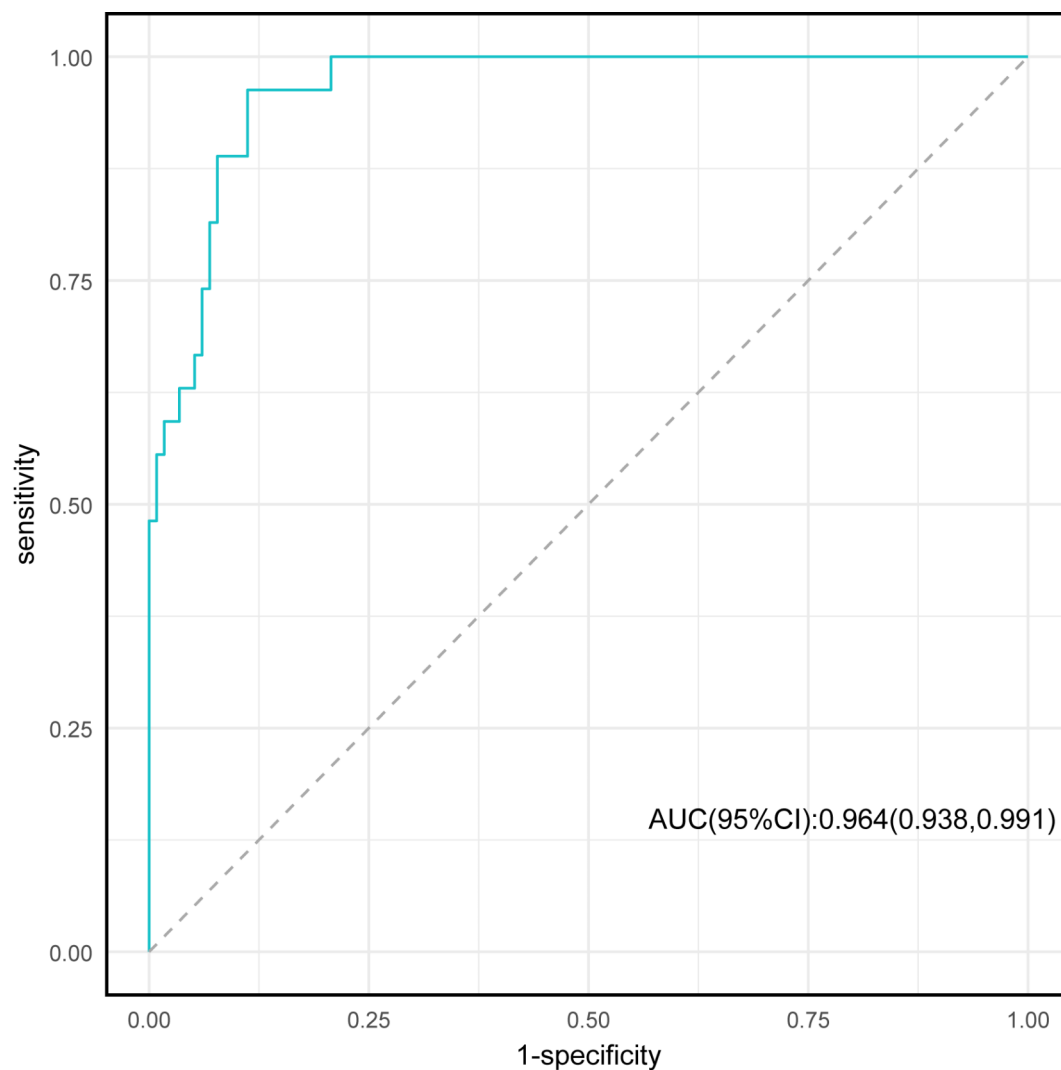


Fig. 4. ROC curve of the logistic regression model.

Sequence	Study	Classification criteria and sample size	Methods	AUC	SEN	SPE	ACC
1	Zhang, X. et al. ^[14]	VAE-NT eyes(59) vs. Normal eyes(142)	Combined tomographic and biomechanical parameters	0.849	0.754	0.871	/
2	Song, P. et al. ^[15]	SKC eyes(31) vs. Normal eyes(35)	Classification And Regression Tree (CART)	0.95	0.903	0.943	0.924
3	Smadja, D. et al. ^[17]	FFKC eyes(47) vs. Normal eye(95)	Automated Decision Tree	/	0.936	0.972	/
4	Ambrósio, R. et al. ^[41]	VAE-NT eyes(551) vs. normal eyes(1680)	TBI_v.2	0.945	0.844	0.901	/
5	Lopes, B. T. et al. ^[42]	VAE-NT eyes(188) vs. stable(298)	Pentacam Random Forest Index(PRFI)	0.968	0.966	0.852	/
6	Our study	SuspectedKC(116) vs. Subclincia KC(28)	Combined tomographic and biomechanical parameters	0.964	0.963	0.888	0.902

Table 4. Classification, methods and AUC of previous relevant studies and this study. SEN: sensitivity; SPE: specificity; ACC: accuracy.

(0.950), and 4 (0.945). This study's sensitivity (0.963) was greater than that of sequences 1–4 (0.754, 0.903, 0.936, 0.844), but its specificity (0.888) was lower than that of sequences 2–4 (0.943, 0.972, 0.901) (Table 4).

The sample sizes for all of the abnormal corneas were greater than those used in this investigation above researches. Importantly, this study's sample size was limited, which might have had an impact on the model's capacity for accurate prediction. Furthermore, biased estimation may arise if the sample data do not accurately reflect the characteristics of the real subclinical and suspected populations. Importantly, the model might not precisely encapsulate the attributes of the complete population. In future investigations, we will gather additional clinical practice samples to improve our model and increase the authenticity and accuracy of model prediction.

In conclusion, the probability of developing keratoconus in suspected cases may be influenced by a combination of morphological and biomechanical factors in Chinese populations. Evaluating parameters such as increased corneal diameter, Belin-related indices, and biomechanical metrics could be instrumental in determining the likelihood of keratoconus, especially in the context of inferior and superior corneal asymmetry. Integrating these factors into the assessment process could improve safety and enhance decision-making in refractive surgery.

Data availability

Data is provided within the manuscript.

Received: 3 October 2024; Accepted: 10 February 2025

Published online: 11 April 2025

References

- Binder, P. S. Ectasia after laser in situ keratomileusis. *J. Cataract Refract. Surg.* **29** (12), 2419–2429. <https://doi.org/10.1016/j.jcrs.2003.10.012> (2003).
- Klyce, S. D. Chasing the suspect: keratoconus. *Br. J. Ophthalmol.* **93** (7), 845–847. <https://doi.org/10.1136/bjo.2008.147371> (2009).
- Henriquez, M. A., Hadid, M. & Izquierdo, L. Jr. A systematic review of subclinical Keratoconus and Forme Fruste Keratoconus. *J. Refractive Surg. (Thorofare N J. : 1995)*. **36** (4), 270–279. <https://doi.org/10.3928/1081597X-20200212-03> (2020).
- Shirayama-Suzuki, M. et al. Longitudinal analysis of corneal topography in suspected keratoconus. *Br. J. Ophthalmol.* **93** (6), 815–819. <https://doi.org/10.1136/bjo.2008.140012> (2009).
- Chen, D. & Lam, A. K. Intrasession and intersession repeatability of the Pentacam system on posterior corneal assessment in the normal human eye. *J. Cataract Refract. Surg.* **33** (3), 448–454. <https://doi.org/10.1016/j.jcrs.2006.11.008> (2007).
- Orucoglu, F. & Toker, E. Comparative analysis of anterior segment parameters in normal and keratoconus eyes generated by scheimpflug tomography. *J. Ophthalmol.* **2015**, 925414. <https://doi.org/10.1155/2015/925414> (2015).
- Luz, A., Lopes, B., Salomão, M. & Ambrósio, R. Application of corneal tomography before keratorefractive procedure for laser vision correction. *J. Biophotonics.* **9** (5), 445–453. <https://doi.org/10.1002/jbio.201500236> (2016).
- Muftuoglu, O., Ayar, O., Hurmeric, V., Orucoglu, F. & Kilic, I. Comparison of multimetric D index with keratometric, pachymetric, and posterior elevation parameters in diagnosing subclinical keratoconus in fellow eyes of asymmetric keratoconus patients. *J. Cataract Refract. Surg.* **41** (3), 557–565. <https://doi.org/10.1016/j.jcrs.2014.05.052> (2015).
- Ma, J., Wang, Y., Wei, P. & Jhanji, V. Biomechanics and structure of the cornea: implications and association with corneal disorders. *Surv. Ophthalmol.* **63** (6), 851–861. <https://doi.org/10.1016/j.survophthal.2018.05.004> (2018).
- Roberts, C. J. & Dupps, W. J. Jr. Biomechanics of corneal ectasia and biomechanical treatments. *J. Cataract Refract. Surg.* **40** (6), 991–998. <https://doi.org/10.1016/j.jcrs.2014.04.013> (2014).
- Nemeth, G. et al. Repeatability of ocular biomechanical data measurements with a Scheimpflug-based noncontact device on normal corneas. *J. Refractive Surg. (Thorofare N J. : 1995)*. **29** (8), 558–563. <https://doi.org/10.3928/1081597X-20130719-06> (2013).
- Ali, N. Q., Patel, D. V. & McGhee, C. N. Biomechanical responses of healthy and keratoconic corneas measured using a noncontact scheimpflug-based tonometer. *Investig. Ophthalmol. Vis. Sci.* **55** (6), 3651–3659. <https://doi.org/10.1167/iov.13-13715> (2014).
- Shetty, R. et al. Understanding the correlation between Tomographic and Biomechanical Severity of Keratoconic Corneas. *Biomed. Res. Int.* **2015** (294197). <https://doi.org/10.1155/2015/294197> (2015).
- Zhang, X. et al. Prognostic nomograms Predicting risk of Keratoconus in very asymmetric ectasia: combined corneal Tomographic and Biomechanical assessments. *Front. Bioeng. Biotechnol.* **10**, 839545. <https://doi.org/10.3389/fbioe.2022.839545> (2022).
- Song, P., Ren, S., Liu, Y., Li, P. & Zeng, Q. Detection of subclinical keratoconus using a novel combined tomographic and biomechanical model based on an automated decision tree. *Sci. Rep.* **12** (1), 5316. <https://doi.org/10.1038/s41598-022-09160-6> (2022).
- Chen, X. et al. Screening of sensitive *in vivo* characteristics for early keratoconus diagnosis: a multicenter study. *Front. Bioeng. Biotechnol.* **11**, 1158299. <https://doi.org/10.3389/fbioe.2023.1158299> (2023).
- Smadja, D. et al. Detection of subclinical keratoconus using an automated decision tree classification. *Am. J. Ophthalmol.* **156** (2), 237–246e1. <https://doi.org/10.1016/j.ajo.2013.03.034> (2013).
- Hu, L. et al. Corneal Vertical and Horizontal Thickness profiles generated by UHR-OCT for suspected and subclinical Keratoconus diagnosis. *J. Refractive Surg. (Thorofare N J. : 1995)*. **37** (7), 438–445. <https://doi.org/10.3928/1081597X-20210330-01> (2021).
- Rabinowitz, Y. S. & Rasheed, K. KISA% index: a quantitative videokeratography algorithm embodying minimal topographic criteria for diagnosing keratoconus. *J. Cataract Refract. Surg.* **25** (10), 1327–1335. [https://doi.org/10.1016/s0886-3350\(99\)00195-9](https://doi.org/10.1016/s0886-3350(99)00195-9) (1999).
- Gomes, J. A. et al. Group of panelists for the Global Delphi Panel of Keratoconus and Ectatic diseases. Global consensus on keratoconus and ectatic diseases. *Cornea* **34** (4), 359–369. <https://doi.org/10.1097/ICO.0000000000000408> (2015).
- Saini, J. S., Saroha, V., Singh, P., Sukhija, J. S. & Jain, A. K. Keratoconus in Asian eyes at a tertiary eye care facility. *Clin. Experimental Optometry.* **87** (2), 97–101. <https://doi.org/10.1111/j.1444-0938.2004.tb03155.x> (2004).
- Awad, E. A., Samra, A., Torky, W. A., El-Kannishy, A. M. & M. A., & Objective and subjective diagnostic parameters in the fellow eye of unilateral keratoconus. *BMC Ophthalmol.* **17** (1), 186. <https://doi.org/10.1186/s12886-017-0584-2> (2017).
- Ruiseñor Vázquez, P. R. et al. Pentacam Scheimpflug tomography findings in topographically normal patients and subclinical keratoconus cases. *Am. J. Ophthalmol.* **158** (1), 32–40e2. <https://doi.org/10.1016/j.ajo.2014.03.018> (2014).
- Song, P. et al. Assessment of corneal pachymetry distribution and morphologic changes in subclinical keratoconus with normal biomechanics. *Biomed. Res. Int.* 1748579. <https://doi.org/10.1155/2019/1748579> (2019).
- Hashemi, H. et al. Best indicators for detecting Keratoconus Progression in children: a Report from the Shahroud Schoolchildren Eye Cohort Study. *Cornea* **41** (4), 450–455. <https://doi.org/10.1097/ICO.0000000000002896> (2022).
- Wahba, S. S., Roshdy, M. M., Fikry, R. R., Abdellatif, M. K. & Abodarahim, A. M. Topographic asymmetry indices: correlation between Inferior Minus Superior Value and Index of Height Decentration. *J. Ophthalmol.* 7875148. <https://doi.org/10.1155/2018/7875148> (2018).
- Shajari, M. et al. Early tomographic changes in the eyes of patients with Keratoconus. *J. Refractive Surg. (Thorofare N J. : 1995)*. **34** (4), 254–259. <https://doi.org/10.3928/1081597X-20180124-01> (2018).
- Alfonso, J. F. et al. Pupil size, white-to-white corneal diameter, and anterior chamber depth in patients with myopia. *J. Refractive Surg. (Thorofare N J. : 1995)*. **26** (11), 891–898. <https://doi.org/10.3928/1081597X-20091209-07> (2010).
- Sanchis-Gimeno, J. A., Sanchez-Zuriaga, D. & Martinez-Soriano, F. White-to-white corneal diameter, pupil diameter, central corneal thickness and thinnest corneal thickness values of emmetropic subjects. *Surg. Radiologic Anatomy: SRA.* **34** (2), 167–170. <https://doi.org/10.1007/s00276-011-0889-4> (2012).
- Xu, G. et al. Distribution of White-to-White corneal diameter and Anterior Chamber depth in Chinese myopic patients. *Front. Med.* **8**, 732719. <https://doi.org/10.3389/fmed.2021.732719> (2021).

31. Shirama, K., Harada, T., Kohda, M. & Hokano, M. Fine structure of melanocytes and macrophages in the harderian gland of the mouse. *Acta Anat.* **131** (3), 192–199. <https://doi.org/10.1159/000146512> (1988).
32. Ding, L., Wang, J., Niu, L., Shi, W. & Qian, Y. Pentacam Scheimpflug Tomography findings in Chinese patients with different corneal diameters. *J. Refractive Surg. (Thorofare N J. : 1995)*. **36** (10), 688–695. <https://doi.org/10.3928/1081597X-20200730-02> (2020).
33. Qin, B. et al. Anterior segment dimensions in Asian and caucasian eyes measured by optical coherence tomography. *Ophthalmic Surg. Lasers Imaging: Official J. Int. Soc. Imaging Eye*. **43** (2), 135–142. <https://doi.org/10.3928/15428877-20120102-03> (2012).
34. Li, Y. et al. Relationship between corneal biomechanical parameters and corneal sublayer thickness measured by Corvis ST and UHR-OCT in keratoconus and normal eyes. *Eye Vis. (London England)*. **8** (1), 2. <https://doi.org/10.1186/s40662-020-00225-z> (2021).
35. Liu, Y., Zhang, Y. & Chen, Y. Application of a scheimpflug-based biomechanical analyser and tomography in the early detection of subclinical keratoconus in Chinese patients. *BMC Ophthalmol.* **21** (1), 339. <https://doi.org/10.1186/s12886-021-02102-2> (2021).
36. Guo, L. L. et al. Comparison of the morphological and biomechanical characteristics of keratoconus, forme fruste keratoconus, and normal corneas. *Semin. Ophthalmol.* **36** (8), 671–678. <https://doi.org/10.1080/08820538.2021.1896752> (2021).
37. Vinciguerra, R. et al. Corneal biomechanics differences between Chinese and caucasian healthy subjects. *Front. Med.* **9**, 834663. <https://doi.org/10.3389/fmed.2022.834663> (2022).
38. Guo, Y., Guo, L. L., Yang, W., Tian, L. & Jie, Y. Age-related analysis of corneal biomechanical parameters in healthy Chinese individuals. *Sci. Rep.* **14** (1), 21713. <https://doi.org/10.1038/s41598-024-72054-2> (2024).
39. Tibshirani, R. & Series, B. Regression shrinkage and selection via the lasso[J]. *Journal of the Royal Statistical Society*, 58(1). (1996). <https://doi.org/10.1111/j.2517-6161.1996.tb02080.x> (1996).
40. Ambrósio, R., Jr, Machado, A. P., Leão, E., Lyra, J. M. G., Salomão, M. Q., Esporcatte, L. G. P., da Fonseca Filho, J. B. R., Ferreira-Meneses, E., Sena, N. B., Jr, Haddad, J. S., Costa Neto, A., de Almeida, G. C., Jr, Roberts, C. J., Elsheikh, A., Vinciguerra, R., Vinciguerra, P., Bühren, J., Kohnen, T., Kezirian, G. M., Hafezi, F., ... Lopes, B. T. Optimized Artificial Intelligence for Enhanced Ectasia Detection Using Scheimpflug-Based Corneal Tomography and Biomechanical Data. *American journal of ophthalmology*, 251, 126–142. <https://doi.org/10.1016/j.ajo.2022.12.016> (2023).
41. Lopes, B. T. et al. Jr. Enhanced Tomographic Assessment to detect corneal Ectasia based on Artificial Intelligence. *Am. J. Ophthalmol.* **195**, 223–232. <https://doi.org/10.1016/j.ajo.2018.08.005> (2018).

Acknowledgements

This study was supported by the project of the Research Fund of the Department of Health of Shandong Province, 202107020443.

Author contributions

Y.S.P. and K.L.L. contributed to the design of the study and confirmation of patient recruitment. Q.Q.F. and T.S. contributed to the manuscript preparation and data analysis. J.F.Z., S.L., H.F.W. and H.L. contributed to the examination and data collection. All authors reviewed the manuscript.

Declarations

Competing interests

The authors declare no competing interests.

Additional information

Correspondence and requests for materials should be addressed to K.L.

Reprints and permissions information is available at www.nature.com/reprints.

Publisher's note Springer Nature remains neutral with regard to jurisdictional claims in published maps and institutional affiliations.

Open Access This article is licensed under a Creative Commons Attribution-NonCommercial-NoDerivatives 4.0 International License, which permits any non-commercial use, sharing, distribution and reproduction in any medium or format, as long as you give appropriate credit to the original author(s) and the source, provide a link to the Creative Commons licence, and indicate if you modified the licensed material. You do not have permission under this licence to share adapted material derived from this article or parts of it. The images or other third party material in this article are included in the article's Creative Commons licence, unless indicated otherwise in a credit line to the material. If material is not included in the article's Creative Commons licence and your intended use is not permitted by statutory regulation or exceeds the permitted use, you will need to obtain permission directly from the copyright holder. To view a copy of this licence, visit <http://creativecommons.org/licenses/by-nc-nd/4.0/>.

© The Author(s) 2025